

Experimental and numerical analysis of discrete damage processes and fluid transport in porous materials

J. Carmeliet & S. Roels

K.U.Leuven, Department of Civil Engineering, Leuven, Belgium

K. de Proft

Royal Military Academy, Civil Engineering Department, Brussels, Belgium.

ABSTRACT: In this paper moisture effects on damage processes are studied experimentally and numerically. In the experimental part the coupling between mechanical and hygric loading during three point bending is investigated using microfocus X-ray projection. This method allows visualizing and quantifying the transport of liquid water in the porous material and the cracks. In the modeling part, two recently developed discrete models, one for simulating discrete damage processes and a second for simulating fluid transport through cracks, are combined in a poromechanical framework.

Keywords: poromechanical, moisture transport, partition-of-unity, discrete model, X-ray projection

1 INTRODUCTION

Moisture in porous materials, such as concrete and rocks, highly influences their mechanical behavior. With increasing moisture saturation, the materials swells, and stiffness and strength both decrease. When the free swelling or shrinkage is hindered, hygric eigenstresses develop and damage in the form of cracks may appear. The cracks are preferential pathways for liquid water leading to an accelerated wetting of the porous material surrounding the crack. The preferential wetting/drying and swelling/shrinking of the area next to the fracture may in turn result in an additional loading of the crack and lead to an acceleration of the damage process.

To include moisture effects in damage processes, poromechanical approaches are coupled to damage-plasticity models (Baggio et al. 2000, Coussy 1995, Grasberger & Meschke 2001, Lewis & Schrefler 1998, Ulm et al. 1999). These damage-plasticity models are continuum models, where localization is handled using smeared or higher order approaches. The penetration of fluids through cracks is usually modeled by an increased permeability in a certain zone, using empirical laws based on average crack widths. First drawback of a continuum model is the necessity of fine FE-

meshes in the vicinity of the crack, resulting in long calculation time. Second, a crack strain over a band governs the damage process rather than a crack width. In this way the continuum model does not take into account the peculiar features of cracks with varying width and connectivity, which may highly influence the resulting permeability. Apart from that, modeling the steep moisture fronts in the fracture often causes numerical instabilities. This is a result of the highly non-linear nature of the constitutive relationships and the strong contrast between physical transport properties of fractures and matrix. To overcome this problem we present a combination of a discrete model simulating cracking and liquid flow in the fracture and a poromechanical continuum model for the uncracked porous matrix. Beforehand, experimental results using microfocus X-ray projection are shown, dealing with the coupling between mechanical and hygric loading during damage processes in porous media.

2 EXPERIMENTS

2.1 *Experimental set-up*

To investigate coupled degradation processes in porous materials a mini test bank device has been developed. The device is small and light enough to be placed on the rotation table of the X-ray

chamber. In this way coupled degradation processes can be followed by X-ray projection measurements or by means of computer tomography. Figure 1 shows the mini test bank device, personal computer and controlling equipment. The test bank device is equipped with a watertight reservoir in which the test samples are placed. In this way it is possible to measure bending, water suction and water suction during bending with the X-ray projection method.



Figure 1. Developed mini test bank device for implementation into the X-ray chamber.

2.2 Experimental results

To illustrate the influence of mechanical loading on the unsaturated moisture transport, Figure 2 gives an example of moisture profiles measured during a combined free suction/bending test on a sample of cellular concrete. This kind of quantitative moisture profiles are obtained by logarithmically subtracting a reference image from images made during the experiment (Roels et al. 2003). In this case the reference image is the image of the dry sample taken during the bending test just after the appearance of a crack in the middle of the sample. The preferential wetting of the sample by the fast water uptake of the fracture is clearly visible. Once the water front in the fracture has reached the opposite side of the sample the fracture acts as an extra water source for the surrounding matrix over almost the total height of the sample.

An example of the influence of moisture on the damage behavior is investigated in a three point bending test on Meule, a French sandstone. In a first part the damage behaviour of a dry and capillary saturated sample is compared. The overall dimensions of the beam are 120x20x18.5 mm³. The supports are situated at a distance of

100 mm. The loading of the sample (middle of top plane) is displacement controlled. The force is measured with a load cell.

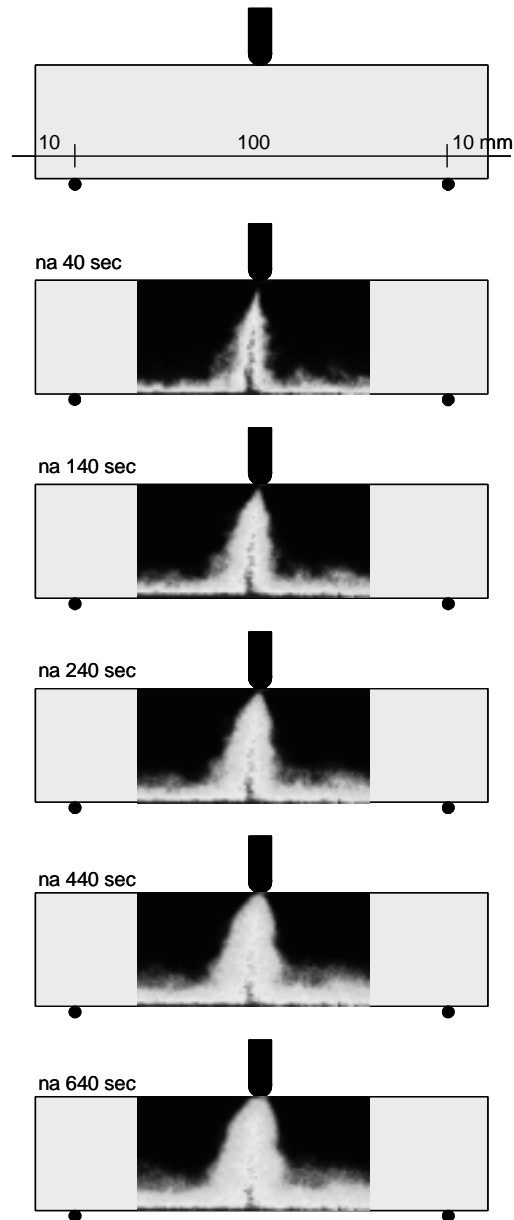


Figure 2. Measured moisture profiles during a combined free suction / bending test on a sample of cellular concrete.

Figure 3 shows the corresponding force as a function of the imposed displacement. A substantial decrease of the maximal force can be noted between dry and capillary saturated state.

Furthermore, the damage behavior becomes more ductile when saturated. In a third bending test, the beam is first loaded to approximately 65% of the maximal loading. From then on, the beam is exposed to a water contact at the bottom side while the loading process continues. Figure 3 shows the measured force versus displacement curve. In a first step a decrease of the loading due to a decrease of the stiffness in the wetted part can be observed. When afterwards the force starts to increase again, soon the decrease of the strength in the wetted zone initiates the damage process leading to failure far below maximum loading.

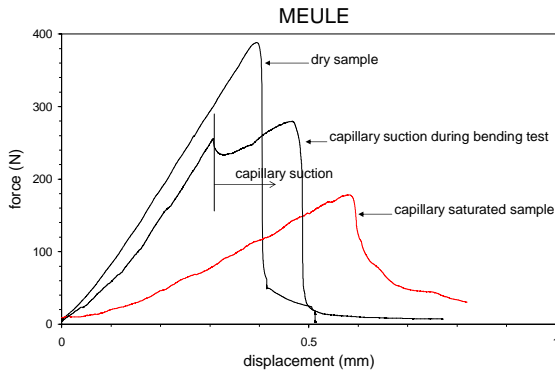


Figure 3. Influence of moisture on the mechanical behavior during bending tests on Meule.

3 NUMERICAL MODEL FOUR COUPLED FLUID DAMAGE PROCESSES

3.1 PU-crack model

In the partition-of-unity (PU) crack model, cracks are modeled as displacement discontinuities, which can freely run through the finite element mesh. The displacement field of a body crossed by m non-intersecting discontinuities (see Fig. 4) is given by

$$\mathbf{u} = \hat{\mathbf{u}} + \sum_{i=1}^m H_{\Gamma_i} \tilde{\mathbf{u}}_i \quad (1)$$

where $\hat{\mathbf{u}}$ and $\tilde{\mathbf{u}}$ are continuous functions and H_{Γ_i} is the Heaviside step function.

The infinitesimal strain field can be found by taking the symmetric gradient of the displacement field:

$$\boldsymbol{\varepsilon} = \nabla^s \hat{\mathbf{u}} + \sum_{i=1}^m H_{\Gamma_i} \nabla^s \tilde{\mathbf{u}}_i + \sum_{i=1}^m \delta_{\Gamma_i} (\tilde{\mathbf{u}}_i \otimes \mathbf{n})^s \quad (2)$$

where \mathbf{n} is the normal to the discontinuity and δ_{Γ_i} is the Dirac delta distribution. The displacement field is implemented within the finite element context using the partition of unity property of the finite element shape functions. When a crack crosses a finite element, nodes are locally enhanced by additional degrees of freedom with the Heaviside step function as an enhancement basis (Wells & Sluys 2001, Moës et al. 1999).

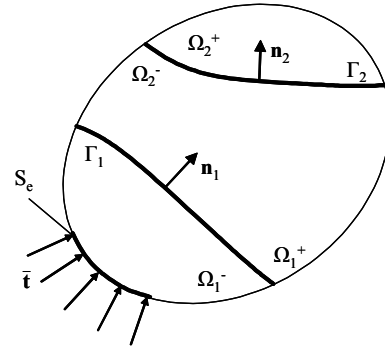


Figure 4. Body Ω crossed by two discontinuities.

Making use of the partition of unity property, the displacement field is obtained by:

$$\mathbf{u} = \mathbf{N}\mathbf{a} + \sum_{i=1}^m H_{\Gamma_i} \mathbf{N}\mathbf{b}_i \quad (3)$$

where \mathbf{N} are the finite element shape functions, \mathbf{a} are the regular degrees of freedom, \mathbf{b} are the enhanced degrees of freedom and m is the number of non-intersecting cracks. The governing finite element equations (De Proft 2003) can be obtained as:

$$\begin{bmatrix} \mathbf{K}_{aa} & \mathbf{K}_{ab_1} & \cdots & \mathbf{K}_{ab_m} \\ \mathbf{K}_{b_1a} & \mathbf{K}_{b_1b_1} & \cdots & \mathbf{K}_{b_1b_m} \\ \vdots & \vdots & \vdots & \vdots \\ \mathbf{K}_{b_ma} & \mathbf{K}_{b_mb_1} & \cdots & \mathbf{K}_{b_mb_m} \end{bmatrix} \begin{Bmatrix} d\mathbf{a} \\ d\mathbf{b}_1 \\ \vdots \\ d\mathbf{b}_m \end{Bmatrix} = \begin{Bmatrix} \mathbf{f}_a^{ext,t+\Delta t} \\ \mathbf{0} \\ \vdots \\ \mathbf{0} \end{Bmatrix} - \begin{Bmatrix} \mathbf{f}_a^{int,t} \\ \mathbf{f}_{b_1}^{int,t} \\ \vdots \\ \mathbf{f}_{b_m}^{int,t} \end{Bmatrix} \quad (4)$$

where

$$\begin{aligned}
\mathbf{K}_{aa} &= \int_{\Omega} \mathbf{B}^T \mathbf{C}^e \mathbf{B} d\Omega \\
\mathbf{K}_{ab_j} &= \int_{\Omega} H_{\Gamma_j} \mathbf{B}^T \mathbf{C}^e \mathbf{B} d\Omega \\
\mathbf{K}_{ab_j} &= \int_{\Omega} H_{\Gamma_j} \mathbf{B}^T \mathbf{C}^e \mathbf{B} d\Omega \\
\mathbf{K}_{b_i b_j} &= \int_{\Omega} H_{\Gamma_i} H_{\Gamma_j} \mathbf{B}^T \mathbf{C}^e \mathbf{B} d\Omega \\
\mathbf{K}_{b_i b_j} &= \int_{\Omega} H_{\Gamma_j} \mathbf{B}^T \mathbf{C}^e \mathbf{B} d\Omega + \int_{\Gamma_j} \mathbf{N}^T \mathbf{D} \mathbf{N} d\Gamma_j
\end{aligned} \tag{5}$$

where \mathbf{C}^e is the continuum elastic material tensor, \mathbf{D} is the material tangent for the discontinuity. It is assumed that the considered element is crossed by discontinuity j and influenced by discontinuity i . More information on implementation can be found in (De Proft 2003, Wells & Sluys 2001).

A traction-separation model governs the behavior at the discontinuity :

$$\begin{aligned}
T_n &= f_t \exp\left(-\frac{f_t}{G_f} \Delta_n\right) \\
T_t &= D_t \Delta_t
\end{aligned} \tag{6}$$

where $\mathbf{T} = \{T_n, T_t\}$ is the traction vector, $\mathbf{\Delta} = \{\Delta_n, \Delta_t\}$ is the separation vector, f_t and G_f are the tensile strength and the mode-I fracture energy of the material and D_t is the elastic stiffness in the tangential direction. A plane stress model models the continuum part.

For the propagation of a discontinuity, a stress criterion is evaluated in the elements in front of the crack tips. When the maximal principal stress exceeds the tensile stress of the material, a new discontinuity is initiated perpendicular to the maximal principal stress direction. After initiation, the nodes of the crossed elements are enhanced.

Discontinuities are allowed to develop at the end of a time step. As was stated by Wells & Sluys (2001) this procedure ensures quadratic convergence of the Newton-Raphson solution process. In order to assure an adequate integration of crossed elements, the integration scheme is changed in these elements. The integration scheme, proposed in Wells & Sluys (2001), is used.

3.2 Unsaturated moisture transport model for cracked materials

To simulate moisture uptake in a fractured porous material, we combine a 1D discrete model for liquid flow in a fracture with a finite element model that solves the unsaturated liquid flow in the porous matrix (Fig. 5). In the discrete fracture flow model the fracture is represented as a row of nodes, connected to each other via flow channels. These flow channels are in fact parallel plates with an aperture equal to the aperture of the fracture segment they belong to. We use the moving front technique to solve the water flow problem in this system. Following Hvistendahl Karlsen et al. (1998) the progress of the moisture front in the fracture is calculated from a combination of a quasi static pressure (Equation 7) and a Darcian flux (Equation 8):

$$\nabla(K(\nabla P_l + \rho_l g \cos \phi)) - S = 0 \tag{7}$$

$$u = \frac{\partial z}{\partial t} = -\frac{K}{\rho_l} (\nabla P_l + \rho_l g \cos \phi) \tag{8}$$

in which K (s) represents the permeability, P_l (Pa) represents the liquid pressure in the fracture segment, g the gravity constant, ρ_l the liquid density (kg/m^3), ϕ the angle of the fracture segment with the vertical ($0^\circ \leq \phi \leq 90^\circ$) and u (m/s) the velocity of the moisture front in the fracture. The latter can be approximated by dz/dt , with dz the progress of the waterfront during the timestep dt (see Fig. 5). In the pressure equation a sink term S is introduced, corresponding to the capillary uptake flow from crack to matrix.

If a fracture segment with aperture b (m) is filled with water, its permeability K (s) is given by (Bear et al. 1993):

$$K = \frac{\rho_l b^2}{12\mu_l} \tag{9}$$

with μ_l the dynamic viscosity of water (kg/m.s). Each timestep Equation 7 and Equation 8 are solved alternatively. First, the pressure equation at time t^n is solved using finite difference schemes. To solve Equation 7 boundary conditions have to be imposed. At the entrance of the fracture ($z=0$) a prescribed liquid pressure corresponding to a water column is assumed. At the top of the waterfilled part, the liquid pressure corresponding to the capillary pressure in the active fracture segment is

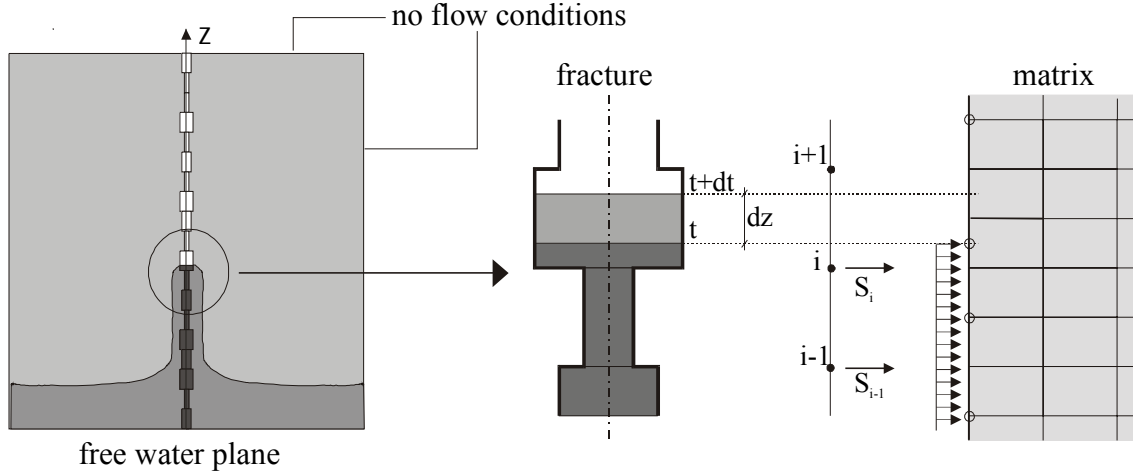


Figure 5. Coupling the discrete fracture model with the FE-model for the analysis of unsaturated moisture transport.

imposed. The capillary pressure is related to the aperture of the active fracture segment by:

$$P_c = 2\sigma_w \cos(\theta)/b \text{ and } P_l = P_g - P_c \quad (10)$$

Here σ_w (N/m) is the surface tension and θ is the contact angle. We assume that every gas pressure build-up rapidly vanishes, so that the gas pressure P_g in the non-filled part of the fracture remains at constant atmospheric pressure. Once the pressures P^n are known in the nodes at the interfaces of the water filled fracture segments, the water front movement dz in the active fracture segment is computed using Equation 8. Since the sink term S in the pressure equation is a function of the water front, a solution can only be achieved by iteration. Each iteration step, this sink term is determined separately by calculating the unsaturated moisture transport in the matrix. To do so, a finite element model based on the continuum approach (Bear & Bachmat 1975, Whitaker 1977) is coupled to the discrete fracture model. Since we limit to unsaturated moisture transfer under isothermal conditions the moisture flow in the matrix can be written by the following differential equation:

$$\frac{\partial w}{\partial t} = -c(P_c) \frac{\partial P_c}{\partial t} = -\nabla^T (\mathbf{k} \nabla P_c) \quad (11)$$

with w (kg/m³) the moisture content, P_c the capillary pressure, $c(P_c)$ the moisture capacity and $\mathbf{k}(P_c)$ the unsaturated permeability of the matrix. For boundary conditions, at the bottom of the matrix a similar condition as for the entrance of the fracture is

applied. At the lateral and top matrix boundaries no flow conditions are assumed. Along the matrix-fracture interface, the capillary pressure corresponding to the calculated liquid pressure field in the crack is imposed as boundary condition. Detailed information and experimental validation of the model can be found in (Roels et al., 2003).

3.3 Numerical model for the coupled analysis

We assume that the moisture transport properties of the material outside the crack do not depend on the mechanical loading, put otherwise the moisture saturation curve as well as the moisture permeability curve as a function of capillary pressure are assumed to be independent of the stresses or strains. The coupling from mechanical loading to moisture transport is described only by geometric aspects of the crack: its length and crack width. This means that the unsaturated moisture analysis in the cracked material can be solved uncoupled from the mechanical analysis.

The coupling between moisture and mechanics is described in a first simple poromechanical approach using the elastic effective stress concept:

$$\boldsymbol{\sigma} = \mathbf{C} \boldsymbol{\varepsilon} + \left(1 - \frac{K}{K_s} \right) \int_{p_c} S(p_c) dp_c \mathbf{I} \quad (12)$$

where $\boldsymbol{\sigma}$ is the stress tensor, $\boldsymbol{\varepsilon}$ is the strain tensor, \mathbf{C} is the constitutive tensor (plane stress), S is the degree of saturation, K , K_s respectively the bulk modulus of the material and of the skeleton, p_c is

the capillary pressure. We assume as initial pressure for fully saturated conditions, $p_{c0} = 0 \text{ N/m}^2$ while for a dry specimen, $p_{c0} = 10^7 \text{ N/m}^2$. The unity tensor is represented by \mathbf{I} . During a mechanical loading step, the capillary pressure is assumed to remain constant. The Young's modulus for Meule sandstone is found to highly depend both on stress and saturation state (Carmeliet & Van Den Abeele, 2002). This dependence is described using the a mesoscopic model called Priesach-Mayergoyz space model, that successfully describes hysteretic non-linear behaviour of rock elasticity with discrete memory, and its dependence on water saturation.

3.4 New finite element formulation

Once a crack appears the finite element formulation of the moisture transport complicates. The outcome of the mechanical analysis is a crack pattern where the cracks are embedded in the finite elements and no nodes are present at the interception of the crack with the finite element borders. The water transport from the crack to the surrounding matrix is described by imposing fixed capillary pressure as boundary at the crack surface. We therefore necessitate nodes at the intersections of crack with finite elements of the matrix. The mechanical model, however, allows cracks to run freely through finite elements. This means that no finite element nodes, which have to be used for imposing the capillary pressures, are located along the fracture. To circumvent this problem, we adapt the finite element mesh for the unsaturated moisture analysis by moving midside nodes to the intersection points of fracture and finite element border. To allow for a correct integration when using intermediate nodes at the moved positions, special shape functions are derived (see Fig. 6).

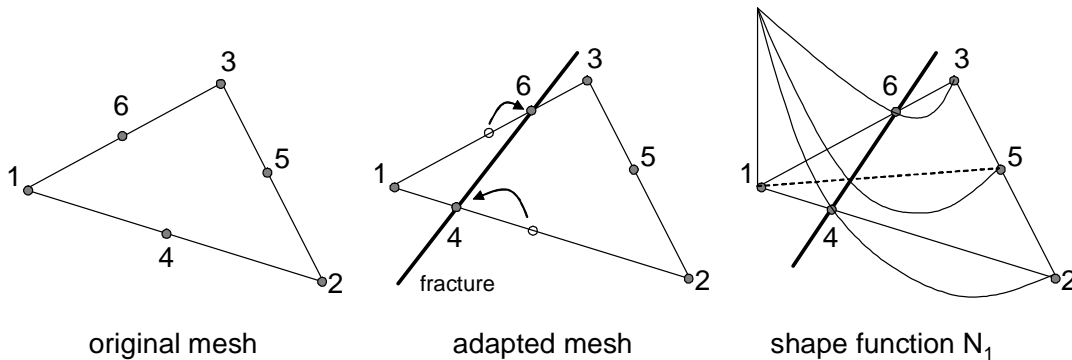


Figure 6. Adapted mesh and example of the corresponding shape functions to impose fixed nodal values along the fracture for the moisture analysis.

Once convergence is achieved in the moisture analysis, the capillary pressures, which serve as input for the mechanical analysis, are update for the original mesh using interpolated values of capillary pressure calculated in the adapted mesh.

4 CONCLUDING REMARKS AND FUTURE WORK

This paper presents a combined discrete approach for describing both fracture development in quasi-brittle materials and unsaturated moisture transport in fractured porous media. The fracture process is modeled by the partition-of-unity (PU) crack model, where cracks are modeled as displacement discontinuities, which can freely run through the finite element mesh. The transport in the fractured material is modeled using a mixed continuum-discrete approach: transport in the crack is described by a moving front model while transport in the matrix is described by a continuum finite element model. The coupling between mechanical and transport phenomena is described by a poromechanical model based on the effective elastic stress concept. In future research we will further enhance the model and validate by coupled transport mechanical experiments.

ACKNOWLEDGEMENT

Funding for this work was provided by KUL PDM/02/138. The measurements with the mini test bank device and the X-ray equipment were performed at the department of Metallurgy and Materials Engineering of the K.U.Leuven.

REFERENCES

- Baggio P., C.E. Majorana and B.A. Schrefler. 2000. Thermo-hygro-mechanical analysis of concrete. *Journal of Engineering Mechanics (ASCE)*, 126:223-242, 2000.
- Bear, J. & Bachmat, Y. 1975. *Introduction to modelling of transport phenomena in porous media*. Dordrecht: Kluwer Academic Publishers.
- Bear, J., Tsang, C-F. & de Marsily, G. 1993. *Flow and contaminant transport phenomena in porous media*. Academic Press, Inc., 1993.
- Carmeliet, J. & Van Den Abeele, K.E.A. 2002. Application of the Preisach-Mayergoyz space model to analyze moisture effects on the nonlinear elastic response of rock. *Geophysical Research Letters* - Vol. 29, No. 7.
- Coussy, O. 1995. *Mechanics of porous continua*. John Wiley & Sons, Chichester.
- De Proft, K. 2003. A combined experimental computational study to discrete fracture of brittle materials. *PhD-thesis, Vrije Universiteit Brussel*.
- Grasberger S. & G. Meschke. Numerical simulation of coupled thermo-hygro-mechanical processes within concrete. In 6th International Conference on Creep, Shrinkage and Durability of Concrete and other Quasi-Brittle Materials (Concreep 6), Cambridge, USA, 2001.
- Hvistendahl Karlsen, K., K. Lie, K.A. Risebro, N.H. & Froyen, J. 1998. A front-tracking approach to a two-phase fluid flow model with capillary forces. *In Situ* 22(1):59-89.
- Lewis R.W. & Schrefler B.A. 1998. *The Finite Element Method in the Static and Dynamic Deformation and Consolidation of Porous Media*. John Wiley & Sons, Chichester.
- Moës, N., Dolbow, J. & Belytschko, T. 1999. A finite element method for crack growth without remeshing. *International Journal of Numerical Methods in Engineering* 46: 131-150.
- Roels, S., Vandersteen, K. & Carmeliet, J. 2003. Measuring and simulating moisture uptake in a fractured porous medium. *Advances in Water Resources* 26: 237-246.
- Ulm, F.-J. J.-M. Torrenti & Adenot F. 1999. Chemo-poroplasticity of calcium leaching in concrete. *Journal of Engineering Mechanics (ASCE)*, 125:1200-1211.
- Wells, G.N. & Sluys, L.J. 2001. A new method for modelling cohesive cracks using finite elements. *International Journal of Numerical Methods in Engineering* 50: 2667-2682.
- Whitaker, S. 1977. Simultaneous heat, mass and momentum transfer in porous media: a theory of drying porous media. *Advances in heat transfer* 119-203.